Pulse Shaping and Shortening by Spatial Filtering of an Induced-Phase-Modulated Probe Wave

A. Dreischuh, E. Eugenieva, and S. Dinev

Abstract—**All-optical deflection and spatial filtering have been used to theoretically model pulse shortening and shaping. Good agreement is obtained with the experimental results of other authors. Pulses with a shortening coefficient of the order of 10, special forms as super-Gaussian, triangular-like, and pairs of pulses with an adjustable peak-to-peak ratio are obtained.**

I. Introduction

In many fields of modern optics (e.g., high-speed optical nonlinear fiber optics, time-resolved spectroscopy) specially shaped optical pulses are desired [1], [2]. In recent years, a variety of techniques for pulse shaping have been developed. One of these techniques includes programmable pulse shaping of femtosecond optical pulses using a spatial filter mask [3]–[6] or a multielement liquid crystal modulator [7] to manipulate the spatially dispersed optical frequency components. Alternative approaches employ intracavity self-phase modulation and temporal pulse shaping in a grating pair compressor [8]–[10], Bragg selectivity of volume holograms [11], or cross-phase-modulation-induced compression of probe pulses by pump pulses [12]. The approach of Kobayashi *et al.* [13], [14] involves a high-speed electrooptic element to deflect and phase-modulate the light passed through, followed by a spatial filter.

The spatial effects of the cross-phase modulation in an optical Kerr-like medium (induced focusing [15]–[17], self- and induced deflection [18]–[20]) are studied extensively, both theoretically and experimentally. These phenomena originate in the induced refractive index change along and across the nonlinear medium and beam cross section, respectively. Recently, the two-beam interference technique has been used for the observation of beams' self-deflection in a three-dimensional Kerr medium [21]. Intensity-dependent self-deflection, combined with far-field spatial filtering, is used for picosecond laser-pulse shortening. This result has stimulated the present analysis.

In this paper we analyze theoretically the spatio-temporal evolution of a probe beam/pulse, when a pump and probe wave copropagate in a nonlinear medium with an initial angular deviation and/or off-axial separation. With this base, we show that a simple spatial filtering of the deflected probe wave can lead to the generation of optical pulses with a special shape and to a reduction of their duration. Good agreement is found with the experimental results of Barthelemy *et al.* [21].

Manuscript received March 9, 1993; revised October 11, 1993. This work was supported by the National Science Foundation, Bulgaria, Under Contract F-206.

The authors are with the Department of Physics, Sofia University, 1126 Sofia, Bulgaria.

IEEE Log Number 9401172.

II. Theoretical Analysis

Let us consider the following arrangement (Fig. 1). Two beams/pulses, the pump at wavelength λ_p and the probe at λ_s enter a planar nonlinear medium of length L_{NL} with an initial off-axis separation r_0 and/or initial angular deviation ϑ. Without loss of generality [19], the nonlinear medium is considered to be resonant and self-focusing. A slit placed at a distance L_0 behind the exit of the nonlinear medium performs a spatial filtering of the deflected phase-modulated probe beam.

Generally, the pump and probe beam/pulse evolution is described by the nonlinear equations

$$i\left[\frac{\partial}{\partial x}+\frac{1}{V_{gp}}\frac{\partial}{\partial t}\right]\psi_p+\frac{1}{2}\beta_{2p}\frac{\partial^2\psi_p}{\partial t^2}+\alpha_p\frac{\partial^2\psi_p}{\partial r^2}+k^{\mathrm{spm}}|\psi_p|^2\psi_p=0, \tag{1a}$$

$$i\left[\frac{\partial}{\partial x}+\frac{1}{V_{gs}}\frac{\partial}{\partial t}\right]\psi_s+\frac{1}{2}\beta_{2s}\frac{\partial^2\psi_s}{\partial t^2}+\alpha_s\frac{\partial^2\psi_s}{\partial r^2}+k^{\mathrm{ipm}}|\psi_p|^2\psi_s=0, \tag{1b}$$

where $V_{gs,p}$ and $\beta_{2s,p}$ are the group velocities and the group-velocity dispersion coefficients for the respective waves, $\alpha_{s,p}=1/(2k_{s,p})$, $k_{s,p}$ are the corresponding wave numbers, and k^{spm} and k^{ipm} are the nonlinear coefficients for self- and induced-phase modulation (SPM and IPM, respectively), related to the nonlinear refractive indexes n_2^{spm} and n_2^{ipm}

$$k^{\mathrm{spm}}=n_2^{\mathrm{spm}}k_p/[2n_{0p}],\quad k^{\mathrm{ipm}}=n_2^{\mathrm{ipm}}k_s/[2n_{0s}].$$

The four-wave frequency mixing terms in (1) could be neglected, since they are not phase matched in the interaction geometry considered [19].

Because of the limited computing resources available, we solved (1) using a modification of the split-step Fourier method, assuming a planar nonlinear medium with a diffraction-nonlimited coordinate r and neglecting the group-velocity mismatch and the group-velocity disper-

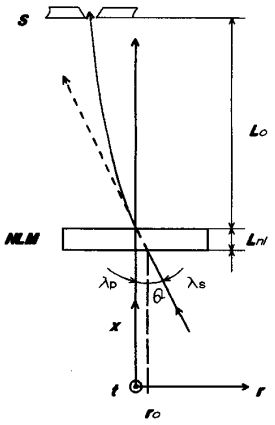

Fig. 1. Interaction geometry considered (NLM—planar nonlinear medium of length L_{NL}, placed at a distance L_o; λ_p, λ_s—wavelengths of the interacting pump and probe waves; ϑ—initial angular probe beam deviation).

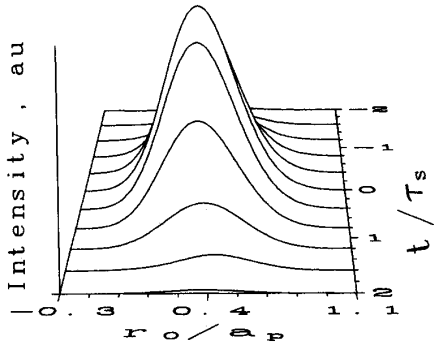

Fig. 2. Spatio-temporal intensity distribution of the probe beam/pulse at the output of the nonlinear medium.

sion. The latter two assumptions enable us to treat time as a parameter at the expense of failing to adequately describe the physical picture of input pulses in the femtosecond time domain. More precisely, L_{NL} and L_o should be much smaller than the dispersive length $L_D = \tau_{s,p}^2/|\beta_{2s,p}|$ and the walk-off length $L_w = (\tau_s^2 + \tau_p^2)^{1/2}/|V_{gs}^{-1} - V_{gp}^{-1}|$. In view of the above restrictions, the femtosecond response of the media with an electronic nonlinearity (e.g., inert gases) could be regarded as instantaneous. Each pulse was divided into $4N$ slices, each having duration $\tau_{slice} = \tau_{s,p}/N$. The minimum slice number required ($N = 50$) was obtained from both energy conservation and the reproducibility of the results against increasing N twice. As a consequence, the initial temporal delay τ_d could be involved adequately if $\tau_d = M\tau_{slice}$, where M is integer. For simplicity $\tau = \tau_s = \tau_p$ is assumed.

A. Qualitative Picture of the Process

The input waves are assumed to be Gaussian in both time and space:

$$\psi_p(r, x = 0, t) = A_{p0} \exp\left\{-\frac{r^2}{a_p^2}\right\} \exp\left\{-\frac{t^2}{2\tau^2}\right\} \quad (2a)$$

$$\psi_s(r, x = 0, t) = A_{s0} \exp\left\{-\frac{(r - r_0)^2}{a_s^2}\right\} \cdot \exp\left\{-\frac{(t - \tau_d)^2}{2\tau^2}\right\}, \quad (2b)$$

where A_i are the slowly varying field amplitudes, a_s and a_p are the beam's radii, and the spatio-temporal coordinate system is taken to be connected with the pump. Fig. 2 shows the probe-wave intensity distribution in both time and space at the exit of the nonlinear medium. The parameters considered are $L_{NL} = 6$ cm, $L_0 = 94$ cm, $a_p = 0.1$ cm, $a_s/a_p = 0.4$, $r_0/a_p = 0.4$, $\tau_d = 0$, $\Delta n = 1/2n_2^{ipm}|A_p|^2 = 5.5 \cdot 10^{-5}$, wavelengths $\lambda_p = 248$ nm and $\lambda_s = 264.4$ nm and the nonlinear medium is Xe at 1 atm.

In a resonant medium if $\lambda_s + \lambda_p$ is near a two-photon resonance, λ_s and λ_p being far from single- and two-photon resonances, one can ignore the pump beam/pulse self-action. Accounting for the pump beam diffraction only simplifies considerably the calculations and reduces the computing time required. Generally, the nonlinear absorption and energy flow, enhanced by a two-photon resonance, could lead to distortions of the interacting wave profiles. In the starting equations (1), the four-wave-mixing terms are omitted, since they are not phase matched. In addition, the nonlinear absorption (proportional to $\{|A_{p0}|^2|A_{s0}|^2\}^{1/2}$) is expected to be low in a pump/probe approximation.

Our attempt to precisely model the experimental results of Barthelemy *et al.* [21] in CS_2 revealed input intensities several times higher than those causing self-focusing instabilities. The two-beam interference pattern used in [21] experimentally allows stabilization of this effect, but is very difficult to model. The parameters of our model, in spite of the resonant interaction, allow a nearly quantitative comparison with the experimental data.

The interplay between diffraction and probe-beam deflection inside the nonlinear medium does not significantly change the intensity distribution straight at the exit of the medium (Fig. 2). Only a small spatial asymmetry near the pulse center can be observed. The picture changes completely when the probe wave passes a distance $L_0 = 94$ cm after the exit of the nonlinear medium (Fig. 3). The spatial oscillatory behavior of the beam at a fixed local time is a manifestation of the spatial analog of the optical wave breaking recently observed [19]. At synchronous pump- and probe- pulse propagation, it is natural to expect a maximum probe-beam deflection near the common pulse center. As seen from the figure, the spatial oscillations are also most pronounced near the pulse maximum. This is to be expected, since the maximum pump intensity in this area induces the highest phase shift on the probe wave. The eventual temporal delay can modify the temporal symmetry of the probe wave. Intensity dependent probe-beam deflection and optical wave breaking can also be expected at coincident but angularly deviated beams at the nonlinear entrance face ($r_0(x = 0) = 0$, $\vartheta \neq 0$). Fig.

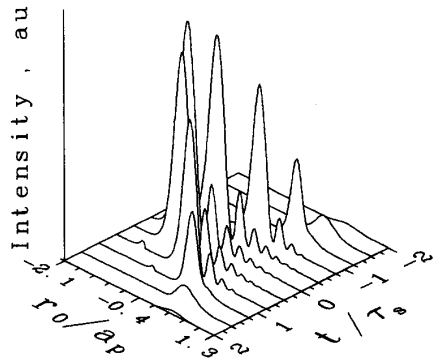

Fig. 3. Intensity distribution of the probe beam/pulse propagated 94 cm from the exit of the nonlinear medium. Note the formation of spatial wave breaking near the pulse center.

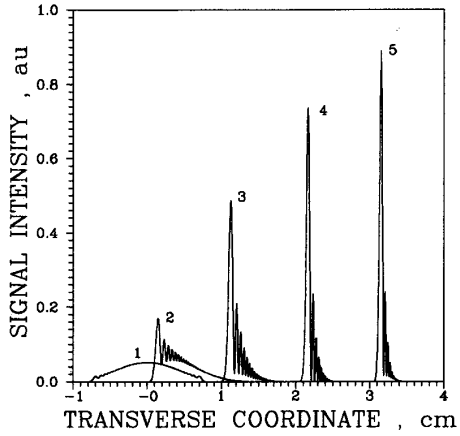

Fig. 4. Transverse intensity distribution of the deflected beam at $t = 0$, initially coincident pump and probe beam centers [$r_0(x = 0) = 0$] and different angular deviation ϑ. 1—$\vartheta = 0°$, 2—$\vartheta = 0.5°$, 3—$\vartheta = 1°$, 4—$\vartheta = 1.5°$, 5—$\vartheta = 2°$.

4 shows the transverse distribution of the central part of the probe pulse (local time $t = 0$ and $\tau_d = 0$) at $\vartheta = 0.5°$ (curve 2), 1° (curve 3), 1.5° (curve 4), and 2° (curve 5). Curve 1 corresponds to a perfect axial and angular alignment of both beams. As seen, the modulation depth of the oscillatory probe-beam wing as well as the intensity of the maximum deviated peak increase with ϑ.

The physical idea to achieve pulse shaping and shortening of the probe pulse is to transmit only a portion of the high-speed optically deflected probe beam/pulse through a spatial filter (e.g., slit). The proper initial angle ϑ between the beams is to be found, as well as the optimum beam diameters and off-axial distance, the initial temporal delay between pulses, slit dimension, and position in order to obtain the desired pulse form and duration.

B. Numerical Analysis

As a first step, we have modeled the probe pulse, resulting from a spatial filtering of the deflected probe beam (later called "signal"). Synchronous pulse propagation is assumed and the model parameters are $a_p = 0.1$ cm, $a_s/a_p = 0.4$, $\Delta n^{\text{ipm}} = 1.1 \cdot 10^{-4}$, $L_{\text{NL}} = 6$ cm, and free-space propagation length $L_0 = 94$ cm. Under these conditions, the slit could be regarded as being placed in the far field. The particular values of L_0 and the slit width are necessary to determine the conditions under which the energy efficiency (compression coefficients, respectively) are calculated. It should be pointed out that the center of gravity of the deflected probe wave and the peak of the beam/pulse do not coincide [22]. In our view, a simple imaging in the focal plane of a lens is not suitable for achieving the actual far-field probe beam profile in front of the slit.

Fig. 5 plots the signal power versus t/τ_s at $\vartheta = 0$ and $r_0(x = 0)/a_p = 0.4$ (dashed curves), as well as at $\vartheta = 1.5°$ and $r_0(x = 0) = 0$ (solid curve). Centering a 100-μm slit at the maximum deviated peak of the probe wave (local time $t = 0$), the signal transmitted (curve 1) has a super-Gaussian (SG) form (power of the super-

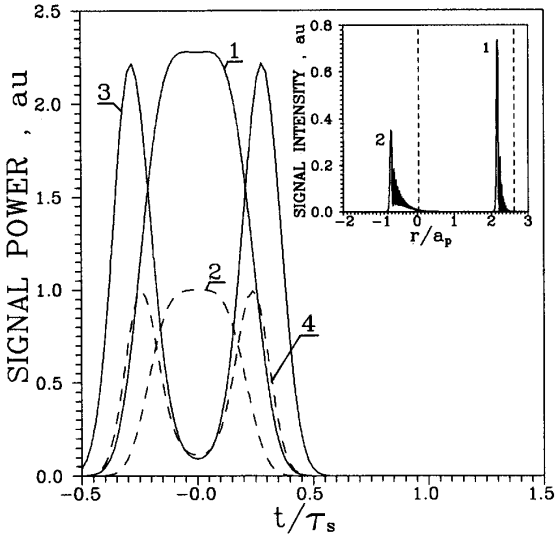

Fig. 5. Signal pulses obtained by the spatial filtering for zero [$r_0(x = 0) = 0$] (1) and nonzero ($r_0/a_p = 0.4$) (2) offset between the centers. A 100-μm slit is centered at the maximum deviated peak at local time $t = 0$. Curves 3, 4—the same, centering the slit at the maximum probe beam deviation for local time $|t| = t_s/4$. Insert: intensity distribution of the deflected probe beam (local time $t = 0$) in front of the slit, corresponding to pulses 1 and 2.

Gaussian $m = 2$). The signal obtained at $\vartheta = 0$ and $r_0(x = 0)/a_p = 0.4$ (curve 2) is approximately 4.7 times shorter than the input probe pulse. This result is in a good agreement with the experimental value of 5 of Barthelemy and co-workers [21], achieved via spatial filtering of a self-deflected beam in a nonresonant Kerr medium by 30 ps input pulses. As seen from Fig. 5, an initial angular deviation ϑ ($\sim 1.5°$) instead of an initial off-axis distance, may lead to a significant (2.25 times) increase of the signal peak power. The insert in Fig. 5 shows the transverse signal intensity distribution of the probe pulse

central part (local time $t = 0$) just in front of the slit. The dashed lines indicate the corresponding probe beam axis in the linear regime of propagation. The comparison is in agreement with the observation in [21] that the greater the deflection, the narrower the transmitted pulse, and that the beam deviation reaches its maximum with the pump pulse intensity and then returns to its initial value (see also, Fig. 3). It should be pointed out once more that the detailed comparison with [21] is difficult due to the complicated highly elliptical pattern of the beam used there to form a spatial soliton. The intensity in the interference fringes along the great axis of the ellipse could only be approximately determined. Nevertheless, the nonlinear deflection angle in our model is 4 mrad, in reasonable agreement with the result of Barthelemy *et al.* of $d\vartheta = n_0^2\Delta n/\vartheta = 4.2$ mrad [21].

From our point of view, the approach introduced in [21] has a large potential for pulse shaping and shortening. Several possible schemes will be analyzed in the following.

At $\tau_d = 0$, the leading and the trailing edges (local times $t \neq 0$) are deflected symmetrically, but less than the central part of the probe pulse. Placing the same slit closer to the probe beam axis in the linear regime, one can select two identical pulses from the less-deflected probe beam parts. Such pulse pairs are plotted in Fig. 5 with a dashed curve ($r_0(x = 0)/a_p = 0.4$, $\vartheta = 0$) and a solid line ($r_0(x = 0) = 0$, $\vartheta = 1.5°$) curve. The 100-μm slit is centered at the maximum deviation for a local time $|t| = \tau_s/4$. Again, the regime with an initial angular deviation seems more attractive for achieving higher signal intensities. All curves in Fig. 5 are normalized to the SG at $\vartheta = 0°$. The energy efficiency of this scheme at the 100-μm slit is 1.8 percent (respectively, 4.8 percent for $\vartheta = 1.5°$) for the SG pulses and 1.6 percent (respectively, 4.0 percent at $\vartheta = 1.5°$) for the twin pulses. Our calculations have shown that for the SG pulses, the signal power energy increases and the signal rise and fall times reduce with increasing the slit width up to 1 mm (energy efficiency of approximately 13.2 percent). These values are comparable to the 15 percent energy efficiency reported in [1], [4], but the square optical pulses generated have rise and fall times below 100 fs and a duration below 1 ps. An advantage of the technique analyzed in the present work is that no initial femtosecond pulses are needed. Shortening starting from longer pulses, an adjustable short pulse, or pulse pair formation could be obtained in the picosecond and subpicosecond ranges. Opening the slit wider results in approaching the initial Gaussian pulse shape. (Note that this is probably due to the neglect of the group-velocity dispersion and requires further analysis at initial pulse durations of less than 10 ps). In the generation of twin pulses, the slit should be kept reasonably narrow in order to achieve higher values of the peak-to-valley contrast. In the case considered, at a 500-μm slit, the two-peak formation practically transforms in a smooth, more or less rectangular pulse.

At a nonzero initial delay τ_d, the physical picture becomes more complicated. The probe pulse symmetry (see Fig. 3) at a local time $t = 0$ is lost. Nevertheless, this offers another possibility for probe pulse shaping and shortening via spatial filtering of the deflected probe wave. Fig. 6 shows the pulses, potentially obtainable at $\tau_d = 0.5\tau_s$ (curve b) and $\tau_d = \tau_s$ (curve c) by fixing a 100-μm slit at the transverse position of the maximum deviated probe peak at $\tau_d = 0$. For comparison, the signal pulse shapes at $\tau_d = 0$ are also presented (curve a). The respective dashed lines represent the case $r_0(x = 0)/a_p = 0.4$, $\vartheta = 0$, the solid lines correspond to $r_0(x = 0) = 0$, $\vartheta = 1.5°$. All curves are normalized to the peak power of the SG pulse at $\vartheta = 0$ and $r_0(x = 0)/a_p = 0.4$. The comparison shows that an initial angular deviation is preferable in order to achieve larger peak powers (respectively, energies). With increasing τ_d the pulses become asymmetric, approaching triangular form. However, as expected, increasing τ_d, the peak power energies tend to decrease. An initial delay τ_d will also change the double-peaked symmetric pulse formation from Fig. 5. Fig. 7 shows the signal pulse shapes, obtained numerically with $r_0(x = 0)/a_p = 0.4$, $\vartheta = 0°$ and a 100-μm slit placed at the maximum deviation for local time $|t| = \tau_s/4$. Curve a corresponds to $\tau_d = 0$ (see Fig. 5, the dashed curve), curve b corresponds to $\tau_d = \tau_s/4$, and curve c corresponds to $\tau_d = \tau_s$. This figure indicates the possibility of achieving pairs of pulses with durations considerably shorter than the initial one, and with an adjustable ratio of their peak powers. Such pairs of pulses may be potentially applicable in studying soliton–soliton interactions and in pump and probe schemes. Qualitatively similar behavior was found in the case of initially centered but angularly deviated pump and probe beams.

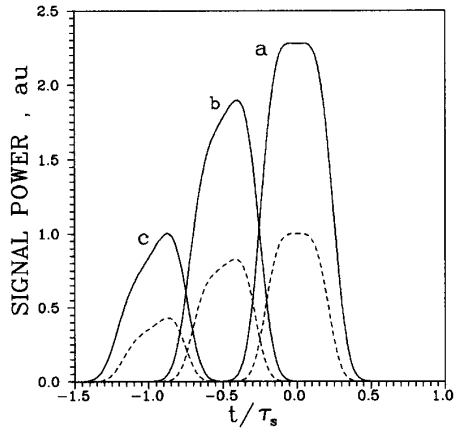

Fig. 6. Evolution of the super-Gaussian signal pulses versus initial pump-to-probe pulse delay τ_d: $a - \tau_d = 0$, $b = \tau_d = 0.5\tau_s$, $c - \tau_d = \tau_s$. Solid curves—zero offset $r_0(x = 0) = 0$ and noncollinear beams $\vartheta = 1.5°$, dashed curves—offset $r_0/a_p = 0.4$ and collinear beams.

Furthermore, we tried to numerically find the maximum probe pulse shortening, e.g., the minimum achievable signal pulse duration after the spatial filtering of the deflected probe wave. Our analysis shows that at $\tau_s = \tau_p$, the optimum initial delay is $\tau_d = \tau_s$. This may be attrib-

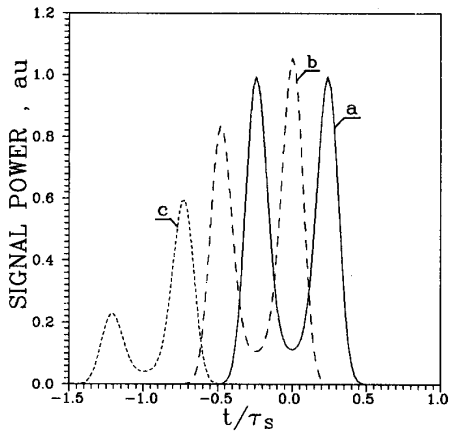

Fig. 7. Evolution of the twin pulses into signal pulse pairs with adjustable peak power ratio. Collinear beams $\vartheta = 0$ and offset $r_0/a_p = 0.4$; slit = 100 μm. Curve $a - \tau_d = 0$; curve $b - \tau_d = \tau_s/4$, curve $c - \tau_d = \tau_s$.

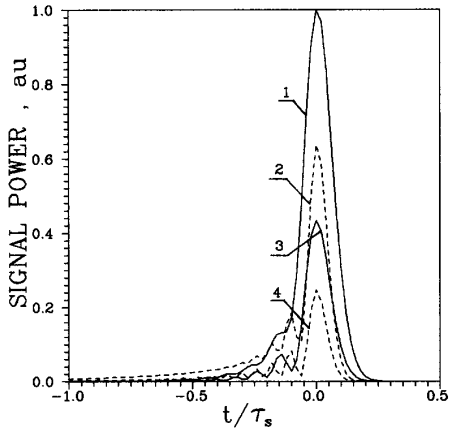

Fig. 8. Signal pulse narrowing at $\tau_d = \tau_s$. Solid curves—$\vartheta = 1.5°$, $r_0 = 0$; dashed curves—$\vartheta = 0$, $r_0/a_p = 0.4$; 1—slit 300 μm, compression 11.8 times, energy conversion 5.1 percent; 2—slit 300 μm, compression 20, energy conversion 2.1 percent 3—slit 100 μm, compression 15, energy conversion 1.7 percent 4—slit 100 μm, compression 22, energy conversion 0.7 percent.

uted to the strong intensity variations of the Gaussian temporal pulse shape assumed at local time $t = \tau_s$. Naturally, for sech- or other types of input pulses the optimum delay may appear to be different. Fig. 8 plots the signal shapes expected after a slit centered at the maximum deviation of the probe at probe local time $t = 0$ for $\tau_d = \tau_s$ ($\tau_s = \tau_p$). The solid curves correspond to $\vartheta = 1.5°$ and perfect initial centering of both beams at the entrance face of the nonlinear medium. The dashed curves are calculated at $r_0(x = 0)/a_p = 0.4$ and zero initial angular deviation. Curves 1 and 2 correspond to a slit width of 300 μm, and respectively, curves 3 and 4 correspond to a slit width of 100 μm. The signal pulses are 10–20 times shorter than the input probe pulses. In all cases the signal duration increases with an increase of the slit width. An initial angular deviation instead of an initial off-axis distance seems preferable in view of the enhanced signal peak power. All curves are normalized to the peak power of the signal at $\vartheta = 1.5°$ and a 300-μm slit width. Qualitatively, the signal pulses have an oscillatory wing, resulting from spatial optical wave breaking. These oscillations become weaker as expressed by increasing the slit width because the picture is spatially integrated over the slit. The compression coefficients and pulse shapes obtained are similar to those predicted for a cross-phase-modulation-induced pulse compression [12]. Characteristic for such pulses are some ringing on the leading side and energy concentration near the trailing side of the pulse.

III. Conclusion

In conclusion, we have theoretically modeled the intensity-dependent probe beam/pulse deflection with a subsequent far-field spatial filtering. The physical mechanism consists of an induced refractive index change along and across the nonlinear medium and beam cross-section, respectively. Two configurations are considered—initially collinear propagation with a suitable off-axis beam distance and initially noncollinear beams with zero radial offset. With this base, schemes for a probe pulse shaping (super-Gaussian of second power, triangular-like and pairs of pulses with an adjustable peak-power ratio and peak-to-peak distance) are proposed. Each of these signal pulse/pulse-pairs has a duration less than the initial probe pulse duration. At a suitably chosen initial pump and probe pulse delay, a probe compression ratio of the order of 10 or more could be achieved. Good agreement with the experimental results of Barthelemy *et al.* [21] is obtained.

An inert gas (Xe) with a femtosecond response time of the electronic nonlinearity and picosecond input pulses are considered. If a Kerr-like nonlinear medium with a picosecond response is used (about 2 ps for CS_2), the phase-modulation effect may not exactly reproduce the temporal profile of the pump pulse and, therefore, should be carefully accounted for. Further considerations and higher computer resources are required to analyze in detail the possibility of such a pulse shaping and compression starting from subpicosecond and femtosecond pulses, as well as under a full cross-modulational coupling between the two beams/pulses.

Acknowledgment

The authors would like to thank D. Kavaldjiev for his contribution during the early stages of this theoretical work.

References

[1] A. M. Weiner, Y. Silberberg, H. Fouckhardt, D. E. Leaird, M. A. Saifi, M. J. Andrejco, and P. W. Smith, "Use of femtosecond square pulses to avoid pulse breakup in all-optical switching," *IEEE J. Quantum Electron.*, vol. QE-25, pp. 2648-2655, 1989, and references therein.

[2] G. Aureli, S. Betfi, G. de Marchis, E. Iannone, and A. Mecozzi, "Theoretical analysis of optical pulse position modulation communication systems using semiconductor lasers," *Opt. Quantum Electron*, vol. 23, pp. 1077-1089 1991.

[3] C. Froehly, B. Colombeau, and M. Vampouille, "Shaping and analysis of picosecond light pulses," in *Progress in Optics XX*, E. Wolf, Ed. Amsterdam, The Netherlands: North-Holland, 1983, pp. 65–153.
[4] A. M. Weiner, J. P. Heritage, and E. M. Kirschner, "High-resolution femtosecond pulse shaping," *J. Opt. Soc. Amer. B*, vol. 5, pp. 1563–1572, 1988.
[5] A. M. Weiner, J. P. Heritage, R. J. Hawkins, R. N. Thurston, E. M. Kirschner, D. E. Leaird, and W. J. Tomlinson, "Experimental observation of the fundamental dark soliton in optical fibers," *Phys. Rev. Lett.*, vol. 61, pp. 2445–2448, 1988.
[6] D. H. Reitze, A. M. Weiner, and D. E. Leaird, "Shaping of wide bandwidth 20 femtosecond optical pulses," *Appl. Phys. Lett.*, vol. 61, pp. 1260–1262, 1992.
[7] A. M. Weiner, D. E. Leaird, J. S. Patel, and J. R. Wullert, "Programmable femtosecond pulse shaping by use of multielement liquid crystal phase modulator," *Opt. Lett.*, vol. 15, pp. 326–328, 1990.
[8] J. Debois, F. Gires, and P. Tournois, "A new approach to picosecond laser pulse analysis, shaping, and coding," *IEEE J. Quantum Electron.*, vol. QE-9, pp. 213–218, 1973.
[9] J. Agostinelli, G. Harvey, T. Stone, and C. Gabel, "Optical pulse shaping with a grating pair," *Appl. Opt.* vol. 15, pp. 2500–2504, 1979.
[10] A. Penzkofer, "Theoretical analysis of pulse shaping of self-phase modulated pulses in a grating pair compressor," *Opt. Quantum Electron.*, vol. 23, pp. 685–702, 1991, and references therein.
[11] D. Brady, A. G.-S. Chen, and G. Rodriguez, "Volume holographic pulse shaping," *Opt. Lett.*, vol. 17, pp. 610–612 (1992); A. M. Weiner, D. E. Leaird, E. G. Paek, "Femtosecond spectral holography," *IEEE J. Quantum Electron.*, vol. 28, pp. 2251–2261, 1992.
[12] G. P. Agrawal, P. L. Baldeck, and R. R. Alfano, "Temporal and spectral effects of XPM on copropagating ultrashort pulses in optical fibers," *Phys. Rev. A*, vol. 40, pp. 5063–5072, 1989.
[13] T. Kobayashi, H. Ideno, and T. Sueta, "Generation of arbitrarily shaped optical pulses in the subnanosecond to picosecond region using a fast electrooptic deflector," *IEEE J. Quantum Electron.*, vol. QE-16, pp. 132–136, 1980.
[14] B. Lee, T. Kobayashi, A. Morimoto, and T. Sueta, "High-speed electrooptic deflector and its application to picosecond pulse generation," *IEEE J. Quantum Electron*, vol. 28, pp. 1739–1744, 1992.
[15] P. L. Baldeck, F. Raccah, and R. R. Alfano, "Observation of self-focusing in optical fibers with picosecond pulses," *Opt. Lett.*, vol. 12, pp. 588–589, 1987.
[16] J. T. Manassah, "Focusing effects of IPM on a probe pulse copropagating in a $\chi^{(3)}$ nonlinear medium," *Opt. Lett.*, vol. 14, pp. 396–398, 1989.
[17] S. Dinev, A. Dreischuh, and A. Naidenov, "Induced waveguiding in a medium with cubic nonlinearity," *J. Opt. Soc. Amer. B*, vol. 8, pp. 2128–2132, 1991.
[18] G. P. Agrawal, "Induced focusing of optical beams in self-defocusing nonlinear media," *Phys. Rev. Lett.*, vol. 64, pp. 2488–2490, 1990.
[19] A. J. Stenz, M. Kauranen, J. Maki, G. P. Agrawal, and R. W. Boyd, "Induced focusing and spatial wave-breaking from XPM in a self-defocusing medium," *Opt. Lett.*, vol. 17, pp. 19–21, 1992.
[20] S. Dinev, A. Dreischuh, and I. Ivanova, "Induced deflection of optical beams in an off-axis geometry," *J. Mod. Opt.*, vol. 39, pp. 667–671, 1992; "——, Spatio-temporal analysis of all-optical streaking," *Appl. Phys. B*, vol. 56, pp. 34–38, 1993.
[21] A. Barthelemy, C. Froehly, S. Maneuf, and F. Reynaud, "Experimental observation of beams' self-deflection appearing with two-dimensional spatial soliton propagation in bulk Kerr material," *Opt. Lett.*, vol. 17, pp. 844–846, 1992.
[22] G. Schwartzlander, Jr., H. Yiu, and A. Kaplan, "Continuous-wave self-deflection effect in sodium vapor," *J. Opt. Soc. Amer. B*, vol. 6, pp. 1317–1325, 1989.

A. Dreischuh, photograph and biography not available at the time of publication.

E. Eugenieva, photograph and biography not available at the time of publication.

S. Dinev, photograph and biography not available at the time of publication.